Adaptive Control of Hysteretic Robotic arm in Operational Space

Somasundar Kannan
SnT- University of Luxembourg, Kirchberg, L-1359 Luxembourg
somasundar.kannan@uni.lu

Serket Quintanar-Guzman
SnT- University of Luxembourg, Kirchberg, L-1359 Luxembourg
serket.quintanar@uni.lu

Souad Bezzaoucha
SnT- University of Luxembourg, Kirchberg, L-1359 Luxembourg
souad.bezzaoucha@uni.lu

Miguel A. Olivares-Mendez
SnT- University of Luxembourg, L-1359 Luxembourg
miguel.olivaresmendez@uni.lu

Holger Voos
SnT- University of Luxembourg, L-1359 Luxembourg
holger.voos@uni.lu

ABSTRACT

The focus of the current article is on Operational Space Control of a single degree of freedom robotic arm with hysteretic joint behaviour due to actuation by a single Shape Memory Alloy (SMA) wire. A Closed Loop Inverse Kinematics Algorithm is used in the outer loop with Adaptive joint control in the inner loop. A composite stability analysis is used to analyse the stability of the closed loop system and finally successfully validated through simulation study.

CCS Concepts

•**Computer systems organization** → **Robotic control;**
•**Computing methodologies** → *Systems theory;*

Keywords

Shape Memory Alloy (SMA) Actuator; Robotic Arm; Hysteresis; Adaptive Control; Inverse Kinematics; Stability.

1. INTRODUCTION

Shape Memory Alloy (SMA) actuators can be classified under special class called as Smart Actuators which posses special advantages compared to conventional actuators such as electric, pneumatic or hydraulic actuators. Some of the key advantages of SMA actuators are that they have high force to mass ratio, noiseless actuation and bio-compatibility etc. Dependeing on the design, shape and form (sheet, wire, spring) SMA actuators have found various applications in medical domain [13, 12, 14], automobile industry [18], motors [17], manipulators [5, 10, 11] and other general purpose actuators [3, 4, 8, 7, 6, 9]. Although SMA actuators have various advantages, they have limited applications due to presence of nonlinear hysteresis behaviour.

In literature different solutions exist for modelling and control of Shape Memory Alloy (SMA) actuators. In [6] we can find a survey of modelling and control methods applicable for SMA actautors.

In [15, 16] sliding mode control was used to perform Joint space control and Operational Space control respectively on a Light weight robotic arm. Here the actuation was performed using two SMA wires.

The contribution of the current article can be summarized as follows:1) Control of Robotic arm actuated by single SMA wire. 2) Operational Space control with inner loop Adaptive control to handle a nonlinear hysteretic joint. 3)And finally Composite stability analysis of the closed loop adaptive control system. The remainder of the paper is organised as follows: First the dynamic of the robotic arm with Shape Memory Alloy (SMA) is briefly presented. Then the operational space control is discussed which includes Closed Loop Inverse Kinematics (CLIK) algorithm in the outer loop and Adaptive Joint Space control in Inner loop. Composite stability analysis of the two loops is discussed followed by validation through simulation.

2. ROBOTIC ARM USING SHAPE MEMORY ALLOY (SMA) WIRE ACTUATOR

Here we will present the mechanical design and Dynamic model of the Robotic arm which uses Shape Memory Alloy (SMA) wire as the actuator.

2.1 Mechanical Design

The mechanical design of the SMA actuated robotic arm can be seen in Figure-1. The main structure of the robotic arm consists of a base followed by two carbon-fibre links with length 100 mm and 150 mm respectively. The second link is a carbon-fibre tube with an end-effector at the end. The

ICMCE '16, December 14-17, 2016, Venice, Italy

DOI: http://dx.doi.org/10.1145/3036932.3036957

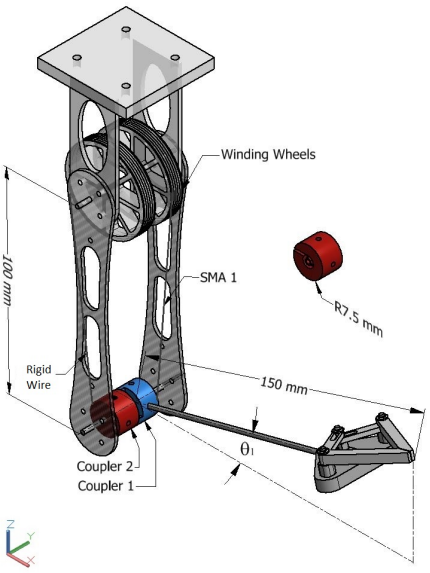

Figure 1: CAD model of the Robotic arm with SMA actuated Joint [15, 16].

second link is actuated through a rotational joint designed in [4]. The rotational joint consist of two couplers of radius 7.5 mm named as coupler-1 and coupler-2 with a torsional spring sandwiched between them. The coupler-1 is attached to the winding wheel through an SMA wire and the coupler-2 is connected to another winding wheel through a rigid wire. When voltage is applied to the SMA wire , the length of the SMA wire shortens and pulls the coupler-1 resulting in displacement of the joint measured as θ. The robotic arm has a maximum displacement angle of 85 degrees in $x-z$ axis. The total weight of the assembly of the given robotic arm measures around 45 g.

2.2 System Modeling

The general schematic of the SMA actuated robotic arm with controller can be seen in Figure-2. The actuator model can be subdivided into the mathematical model of the SMA wire, the kinematics and Dynamics of the robotic arm. Further the nonlinear model of the SMA wire can be subdivided into Thermal Dynamics, Phase Transformation and wire Constitutive model. For further details of the nonlinear model of the SMA wire please refer to [15] and [16]. The input to the closed loop system is cartesian position of the end-effector, while the Operational Space control which consist of Closed Loop Inverse Kinematic Algorithm generates the reference trajectory for the Joint Space inner control. The inner joint space controller generates the required voltage to actuate the SMA wire in-turn rotating the joint of the manipulator. Next we will describe the kinematics and dynamics of the robotic arm.

2.2.1 Kinematics and Dynamics.

In this section we will briefly describe the kinematics and dynamics.

Kinematic Model. The kinematics of the SMA actuator

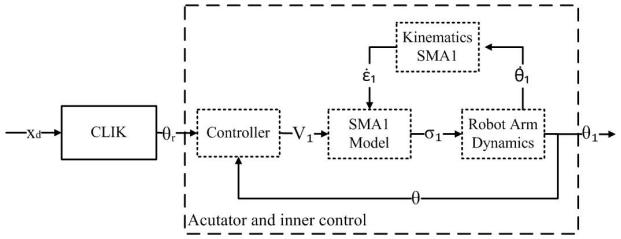

Figure 2: Control scheme of SMA actuated robotic arm

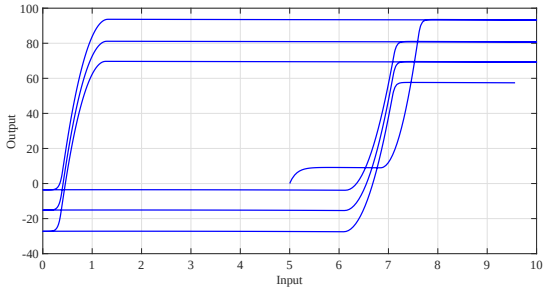

Figure 3: Open-Loop Hysteresis Behaviour in the Robotic Arm, with Input reference voltage and Output Rotational Joint displacement in degrees.

is given by

$$\dot{\varepsilon} = -\frac{\phi\dot{\theta}}{l_0} \tag{1}$$

where $\dot{\varepsilon}$ is the strain rate of the SMA wire, ϕ is the radius of the coupler, l_0 the initial length of the SMA wire and $\dot{\theta}$ is the angular velocity of the coupler-1. Here it should be noted that only the coupler-1 is rotating and the coupler-2 is rigidly attached to the winding wheel through a rigid wire.

Dynamics. The dynamic model of the robotic arm actuated by SMA wire can be given by

$$M(\theta)\ddot{\theta} + V_m(\theta,\dot{\theta})\dot{\theta} + g(\theta) + F_d\dot{\theta} + \Phi(\theta,\theta_r) = \tau_w \tag{2}$$

where θ, $\dot{\theta}$, $\ddot{\theta}$ are the position, velocity and acceleration of the systems, $M(\theta)$ is the inertia matrix, $V_m(\theta,\dot{\theta})$ is the centripetal-coriolis matrix, $g(\theta)$ is the gravity term, F_d is the viscous coefficient term, $\Phi(\theta,\theta_r)$ is the nonlinear hysteretic term. Here τ_w is the input torque applied to the manipulator joint by the SMA wire which can be computed using

$$\tau_w = F_w\phi = A\sigma\phi \tag{3}$$

where σ is the stress in the SMA wire, ϕ is the radius of the coupler, $A = 4.9 \times 10^{-8}\ m^2$ is the transversal area of the SMA wire. The complete dynamic model is simulated in the Simmechanics environment of Matlab/Simulink. Further details of the model can be obtained from [15] and [16]. The nonlinear hysteresis problem present in the joint of the robotic arm can be seen in the Figure-3.

3. OPERATIONAL SPACE CONTROL

The operational space control is discussed here. The operational space control can be further subdivided into outer

loop Closed Loop Inverse Kinematics and Inner loop Adaptive Joint control.

3.1 Closed Loop Inverse Kinematics

The outer loop which consist of Closed Loop Inverse Kinematics algorithm is discussed here. The forward kinematics can be defined by

$$x_e = f(\theta) \tag{4}$$

and the velocity as below

$$\dot{x}_e = J(\theta)\dot{\theta} \tag{5}$$

where $f(\theta)$ is the forward kinematics and $J(\theta)$ is the jacobian. Let us define the desired end-effector error as follows

$$e_o = x_d - x_e \tag{6}$$

where x_d is the desired end-effector position and x_e is the true end-effector position. Let us choose the Lyapunov function

$$V_o = \frac{1}{2} e_o^T K_o e_o \tag{7}$$

where K_o is a symmetric positive definite matrix and V_o is positive definite. Now differentiating V_o with respect to time we get

$$\dot{V}_o = e_o^T K_o \dot{x}_d - e_o^T K_o \dot{x}_e \tag{8}$$

Substitute $\dot{x}_e = J\dot{\theta}$ in the above equation and using $\dot{\theta} = J^T K_o e_o$ [1] we get

$$\dot{V}_o = e_o^T K_o \dot{x}_d - e_o^T K_o J J^T K_o e_o \tag{9}$$

$$= -e_o^T K_o \left[J J^T K_o e_o - \dot{x}_d \right] \tag{10}$$

$$\leq -\lambda_1 ||e_o|| \left[\lambda_1 \lambda_2 ||e_o|| - ||\dot{x_d}|| \right]. \tag{11}$$

The error dynamic system $\dot{e}_o$ is stable if the following condition (12) is satisfied

$$||\dot{x}_d|| \leq \lambda_1 \lambda_2 ||e_o|| \tag{12}$$

where we have $\lambda_1 = \lambda_{max}\{K_o\}$ and $\lambda_2 = \lambda_{max}\{J^2\}$ and λ_{max} is the respective maximum eigen value.

3.2 Adaptive Joint Control

Here we will briefly present the Inner loop Joint control.We will utilize an adaptive control solution based on [2]. Let us define the joint tracking error $e(t) \in \mathbb{R}^n$ as follows

$$e = \theta_d - \theta \tag{13}$$

where $\theta_d(t) \in \mathbb{R}^n$ is the desired joint angle position. We will need the filtered tracking error $r(t) \in \mathbb{R}^n$ given as [2]

$$r = \dot{e} + \alpha e \tag{14}$$

where α is a known constant. After extensive computation [2] the open loop dynamics in terms of r can be written as

$$M(\theta)\dot{r} = -V_m(\theta, \dot{\theta}) r + \gamma - \tau \tag{15}$$

where we have

$$\gamma = M(\theta)(\ddot{\theta}_d + \alpha \dot{e}) + V_m(\theta, \dot{\theta})(\dot{\theta}_d + \alpha e) + g(\theta) + F_d \dot{\theta} + \Phi(\theta, \theta_r) \tag{16}$$

Based on (15) let us choose the following control input

$$\tau = \hat{\gamma} + Kr \tag{17}$$

where K is the control gain and $\hat{\gamma}$ is the estimate of γ. The value of $\hat{\gamma}$ is updated using

$$\dot{\hat{\gamma}} = \Gamma^{-1} r \tag{18}$$

where Γ is a positive definite adaptation gain. Using (15) and (17) we have the closed loop system for r given as

$$M(\theta)\dot{r} = -V_m(\theta, \dot{\theta}) r - Kr + \tilde{\gamma} \tag{19}$$

where $\tilde{\gamma} = \gamma - \hat{\gamma}$. Now let us first choose the Lyapunov function suitable for our system [2]

$$V_i = \frac{1}{2} r^T M(\theta) r + \frac{1}{2} \tilde{\gamma}^T \Gamma \tilde{\gamma}. \tag{20}$$

Differentiating V with respect to time we get

$$\dot{V}_i = \frac{1}{2} r^T \dot{M}(\theta) r + r^T M(\theta) \dot{r} + \frac{1}{2} \tilde{\gamma}^T \Gamma \dot{\tilde{\gamma}} \tag{21}$$

After substitution of closed loop equation (19) we get

$$\dot{V}_i = \left[\frac{1}{2} r^T \dot{M}(\theta) r - r^T V_m(\theta, \dot{\theta}) r \right] - r^T K r + \tilde{\gamma}^T \left(r + \Gamma \dot{\tilde{\gamma}} \right), \tag{22}$$

using the property [2]

$$\frac{1}{2} r^T \dot{M}(\theta) r - r^T V_m(\theta, \dot{\theta}) r = 0 \tag{23}$$

and substituting

$$\dot{\tilde{\gamma}} = -\Gamma^{-1} r \tag{24}$$

since γ is a constant based on our assumption. With further simplification we get

$$\dot{V}_i = -r^T K r \leq -\lambda_3 ||r||^2 < 0 \tag{25}$$

where $\lambda_3 = \lambda_{min}\{K\}$ is the minimum eigen value of the matrix. From (25) we can conclude that the closed loop system using control law (17) and adaptive law (18) is asymptotically stable since the time derivative of the Lyapunov function is negative.

3.3 Composite Stability

Here we will briefly discuss the stability of the composite system involving the outer-loop Closed Loop Inverse Kinematics and the inner loop joint control. Let us define the composite Lyapunov function

$$V = V_o + V_i \tag{26}$$

where V_o and V_i are given in (7) and (20) respectively. Based on (11) and (25) the time derivatives can be given by

$$\dot{V} = -e^T K_o \left[J J^T K_o e - \dot{x}_d \right] \tag{27}$$

$$+ \left[\frac{1}{2} r^T \dot{M}(\theta) r - r^T V_m(\theta, \dot{\theta}) r \right] - r^T K r + \tilde{\gamma}^T \left(r + \Gamma \dot{\tilde{\gamma}} \right) \tag{28}$$

$$\leq -\lambda_1 ||e|| \left[\lambda_1 \lambda_2 ||e|| - ||\dot{x_d}|| \right] - \lambda_3 ||r||^2 \tag{29}$$

As stated in the previous subsection-3.1 the stability condition is satisfied as long as $||\dot{x}_d|| \leq \lambda_1 \lambda_2 ||e_o||$. Hence the composite system including outer-loop Closed Loop Inverse Kinematics and the inner-loop Adaptive Joint control is asymptotically stable since time derivative of the composite Lyapunov function ($\dot{V}$) is negative.

4. SIMULATION

Simulation study is performed here by applying the above discussed operational space control to the hysteretic manipulator. For the purpose of simulation the control law in (17) is used along with the adaptation law (18) for the inner control loop of the Joint. The reference to the inner loop is generated by the Closed Loop Inverse Kinematic (CLIK) algorithm discussed in Section-3.1. The controller parameters used in the simulation are $K = 20$, $\alpha = 2$ and $\Gamma = 0.2$ for the joint space control and for the CLIK algorithm the control gain

$$K_o = \begin{bmatrix} 300 & 0 \\ 0 & 300 \end{bmatrix}. \tag{30}$$

The simulation results can be seen in Figure-4, Figure-5, Figure-6, Figure-7, Figure-8 and Figure-9.

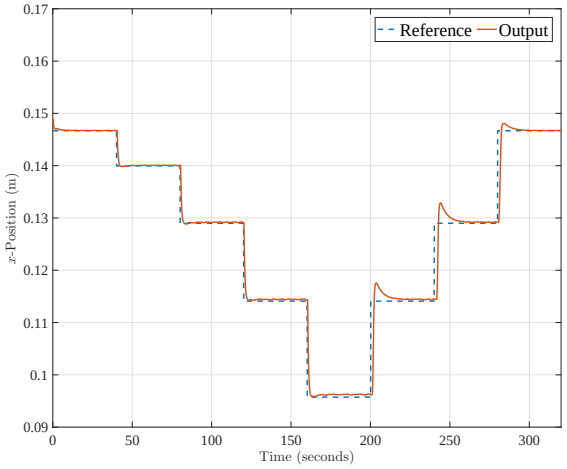

Figure 4: End-Effector Position response in x-axis.

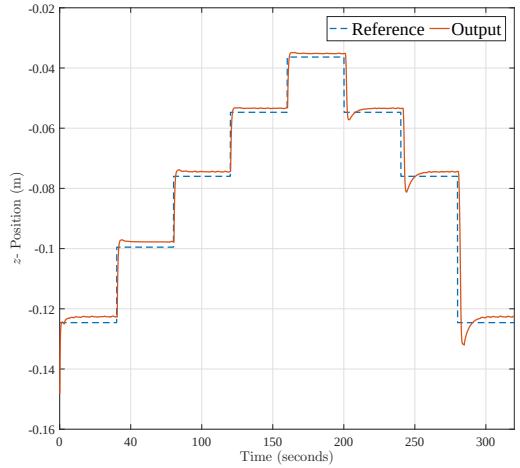

Figure 5: End-Effector Position response in z-axis.

The End-effector position response in x-axis can be seen in Figure-4, while the position response in z-axis can be seen in Figure-5. The x and z axis position tracking error can be seen in Figure-6. In Figure-7 the control input to the

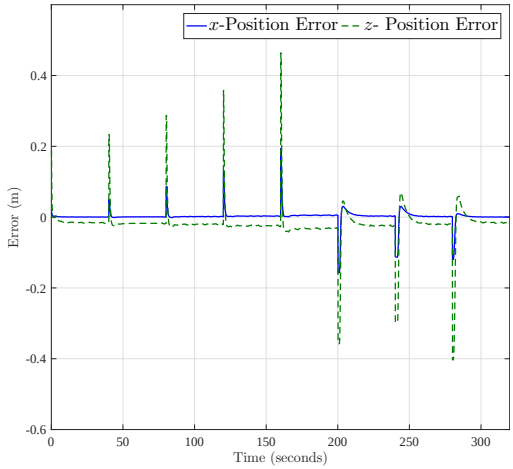

Figure 6: End-Effector x and z Position Tracking Error

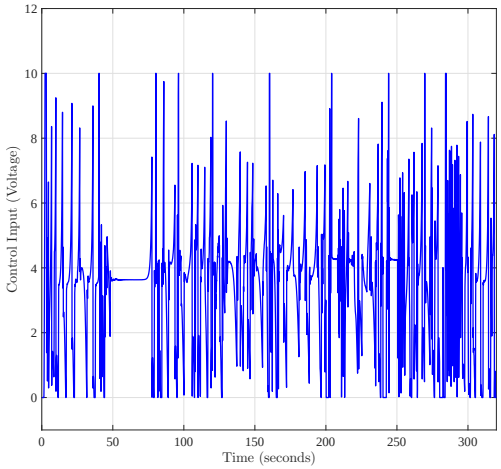

Figure 7: Control Input.

actuator can be seen. In the inner control loop the joint space tracking response can be seen in Figure-8 while the adaptive control gain in the inner loop can be seen in Figure-9. The maximum overshoot of 2.9 % in the x-axis tracking can be seen in Figure-4 at around 200 seconds. Similarly the maximum undershoot of 5.9 % can be seen in z-axis tracking in Figure-5 at around 300 seconds. In the x-axis tracking the Mean and RMS (Root Mean Square) tracking error are 1.864×10^{-3} m and 1.991×10^{-2} m respectively. In the z-axis tracking the Mean and RMS error are 1.972×10^{-2} m and 5.692×10^{-2} m respectively.

5. CONCLUSION

In the current article the modelling and control of a hysteretic robotic arm actuated by Shape Memory Alloy (SMA) wire was discussed. The target of the control design was to perform control in operational space. Hence a Closed Loop Inverse Kinematics algorithm was used in the outer-loop while an adaptive control algorithm was used in the inner-loop for joint space control to handle the hysteresis.

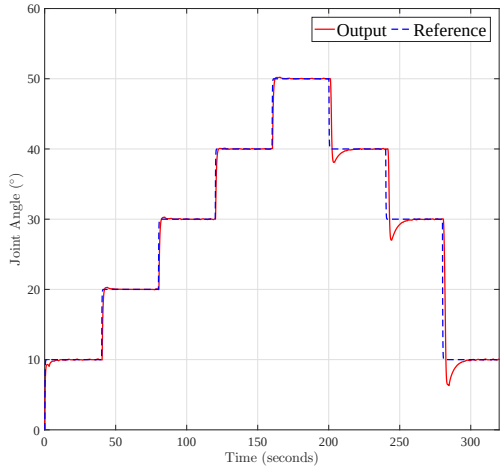

Figure 8: Manipulator Joint Position Response.

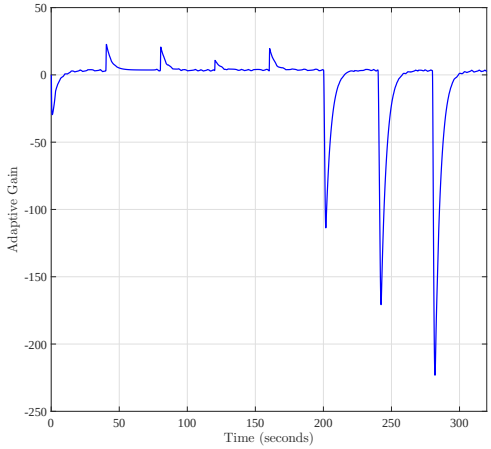

Figure 9: Response of Adaptive gain.

Simulation studies were successfully performed for reference tracking of the end-effector and analysed briefly. The future perspectives of the current research includes the experimental implementation of the proposed methods.

6. REFERENCES

[1] B.Siciliano, L. Sciavicco, L. Villani, and G. Oriolo. *Robotics:Modelling, Planning and Controls*. Springer, 2009.

[2] M. S. de Queiroz, D. M. Dawson, S. P. Nagarkatti, and F. Zhang. *Lyapunov-Based Control of Mechanical Systems*. Springer Science & Business Media, 2012.

[3] M. H. Elahinia and H. Ashrafiuon. Nonlinear Control of a Shape Memory Alloy Actuated Manipulator. *Journal of Vibration and Acoustics*, 124(4):566, 2002.

[4] Z. Guo, Y. Pan, L. B. Wee, and H. Yu. Design and control of a novel compliant differential shape memory alloy actuator. *Sensors and Actuators A: Physical*, 225:71–80, apr 2015.

[5] M. Hulea and C. F. Caruntu. Spiking neural network for controlling the artificial muscles of a humanoid robotic arm. pages 163–168, 2014.

[6] S. Kannan. *Modélisation et Commande dActionneurs à Alliage à Mémoire de Forme*. PhD thesis, l'École Nationale Supérieure d'Arts et Métiers, 2011.

[7] S. Kannan, C. Giraud-Audine, and E. Patoor. Control of shape memory alloy (sma) actuator using series-parallel model reference adaptive control (mrac). In *ASME 2009 Conference on Smart Materials, Adaptive Structures and Intelligent Systems*, pages 441–450. American Society of Mechanical Engineers, 2009.

[8] S. Kannan, C. Giraud-Audine, and E. Patoor. Laguerre model based adaptive control of antagonistic shape memory alloy (sma) actuator. In *SPIE Smart Structures and Materials+ Nondestructive Evaluation and Health Monitoring*, pages 764307–764307. International Society for Optics and Photonics, 2010.

[9] S. Kannan, C. Giraud-Audine, and E. Patoor. Application of laguerre based adaptive predictive control to shape memory alloy (sma) actuator. *ISA Transactions*, 52(4):469 – 479, 2013.

[10] A. Khodayari, M. Talari, and M. M. Kheirikhah. Fuzzy PID controller design for artificial finger based SMA actuators. *IEEE International Conference on Fuzzy Systems*, pages 727–732, 2011.

[11] J. Ko, M. B. Jun, G. Gilardi, E. Haslam, and E. J. Park. Fuzzy PWM-PID control of cocontracting antagonistic shape memory alloy muscle pairs in an artificial finger. *Mechatronics*, 21(7):1190–1202, 2011.

[12] X. Liu, Y. Wang, D. Yang, and M. Qi. The effect of ageing treatment on shape-setting and superelasticity of a nitinol stent. *Materials Characterization*, 59(4):402–406, 2008.

[13] F. Nematzadeh and S. Sadrnezhaad. Effects of material properties on mechanical performance of nitinol stent designed for femoral artery: Finite element analysis. *Scientia Iranica*, 19(6):1564 – 1571, 2012.

[14] N. Pandis and C. P. Bourauel. Nickel-titanium (niti) arch wires: the clinical significance of super elasticity. In *Seminars in Orthodontics*, volume 16, pages 249–257. Elsevier, 2010.

[15] S. Quintanar-Guzman, S. Kannan, M. A. Olivares-Mendez, and H. Voos. Lightweight robotic arm actuated by shape memory alloy (sma) wires. In *IEEE International Conference on Electronics, Computers and Artificial Intelligence*, pages –. IEEE, 2016.

[16] S. Quintanar-Guzman, S. Kannan, M. A. Olivares-Mendez, and H. Voos. Operational space control of a light weight robotic arm actuated by shape memory alloy (sma) wires. In *Smart Materials, Adaptive Structures and Intelligent Systems (ASME-SMASIS 2016)*, pages –. ASME, 2016.

[17] S. Quintanar-Guzmán, J. Reyes-Reyes, and M. d. c. Arellano-Sánchez. Modelado y control de un sistema electrotérmico-mecánico móvil basado en alambres musculares. In *XVI Congreso Latinoamericano de Control Automático, CLCA 2014*, pages 834–839. Asociación de México de Control Automático, 2014.

[18] E. A. Williams, G. Shaw, and M. Elahinia. Control of an automotive shape memory alloy mirror actuator. *Mechatronics*, 20(5):527–534, 2010.